Hydrodynamical analysis of proton-nucleus collision data at 200 GeV

Naohiko Masuda*
Department of Physics, University of Marburg, D-355 Marburg, West Germany and Institute for Theoretical Physics, University of Leuven, B-3030 Heverlee, Belgium

Richard M. Weiner
Department of Physics, University of Marburg, D-355 Marburg, West Germany
(Received 12 October 1976; revised manuscript received 25 July 1977)

Numerical results of the one-dimensional hydrodynamical model of proton-nucleus collisions are applied to the data on p-H_2, p-Al, p-emulsion, and p-Ag collisions at 200 GeV. We find that the hydrodynamical model with a velocity of sound of excited hadronic matter of $u \simeq 1/(7.5)^{1/2}$ can adequately describe most of the experimental facts connected with the rapidity distributions of charged particles. An essential assumption in our approach is that the (experimentally unknown) number of fast recoiling protons, which experimentally are counted as shower-particle tracks, grows as the target nuclear size grows and that their distribution in rapidity is proportional to the pion distribution obtained from hydrodynamics. A comparison with the predictions of other theoretical models is also made.

In two previous papers,[1,2] we made an extensive study of many aspects of proton-nucleus collisions at high energies based on Landau's hydrodynamical model.[3] In the first paper[1] (hereafter referred to as I) we reexamined Belenkij and Milekhin's hydrodynamical prediction[4] for the multiplicity ratio R of proton-nucleus collision vs proton-proton collision by considering a smaller value for the velocity of sound of excited hadronic matter and the diffuse edge of the nuclear density distribution. We found that with the velocity of sound $u \sim 1/\sqrt{6} \sim (0.1)^{1/2}$ corresponding to an interacting Bose gas and with a reasonable parametrization of the diffuse edge effect, the hydrodynamical model can describe satisfactorily the currently available experimental data on R. In that paper we derived an exact formula for the multiplicity ratio R for a collision of a proton of diameter d and a one-dimensional target tunnel of length l as a function of u and l/d. In the second paper[2] (referred to as II) we studied rapidity distributions of secondary particles and energy fluxes. For this purpose we solved the one-dimensional relativistic hydrodynamical equations with appropriate boundary conditions for arbitrary target tunnel length. Numerical studies for the representative target nuclei, H, Al, Ni, and W, with velocity of sound $u = 1/\sqrt{3}$ of the relativistic ideal Bose gas and $u = 1/\sqrt{6}$ and $1/(7.5)^{1/2}$ of interacting Bose gases, were made. New effects specific to proton-nucleus collisions were predicted.

However, in that second paper we did not attempt to fit the experimental data with our results since there were not enough data available. Recently new data on proton-nucleus collisions with fixed targets at 200 GeV by Busza *et al.*[5] have become available in addition to the earlier data by Florian *et al.*[6] Although the target nuclei studied in the above two papers are different, the data show consistent trends in many aspects and they are also consistent with the data from earlier nuclear emulsion experiments.[7] In this paper we analyze the data by Busza *et al.* on the rapidity distribution of charged particles in proton-nucleus collisions at 200 GeV in terms of the one-dimensional hydrodynamical model, the solutions of which were presented in II. The data[5] on the rapidity distributions of charged particles exist for the target nuclei with $\bar{\nu}$ (the average thickness in units of the mean free path of the incident particle) = 1 (hydrogen), 2, 2.5 (emulsion), 3(Ag), and 4. The target $\bar{\nu} = 2$ may approximately correspond to the Al target since $\bar{\nu}$ for Al is 1.95. The case $\bar{\nu} = 4$ will not be discussed in this paper since our numerical calculations do not apply for very large nuclei.

We convert a collision problem of a proton and a nucleus with a spherical shape into that of a proton and a one-dimensional nuclear tunnel whose length is determined from the average impact parameter as in II. A geometrical averaging over impact parameter of collisions between a proton and a nucleus of mass number A results in the average impact parameter

$$b_A = \tfrac{2}{3} a_0 A^{1/3} \tag{1}$$

and the corresponding average tunnel length

$$L_A = \frac{2\sqrt{5}}{3} a_0 A^{1/3} , \tag{2}$$

where $a_0 = a_\pi = 1/m_\pi$.

In the equal-velocity frame (evf) for a highly relativistic collision the system consists of two Lorentz-contracted particles, namely the incident

proton of diameter

$$d = 2a_\pi \frac{M}{E} \tag{3}$$

in the direction of the collision axis and the target of diameter

$$l = L_A \frac{M}{E} \ . \tag{4}$$

in the same direction. E in Eqs. (3) and (4) is the energy of the incident proton in evf and is equal to the energy of each nucleon inside the target and M is the nucleon mass.

The details of compression and excitation of hadronic matter accompanied by shock wave propagation and subsequent hydrodynamical expansion were explained in II. The solutions of the fluid motion in the expansion stage were obtained in II for both cases of target tunnel length $l \leq l_c$, and $l > l_c$ where the critical tunnel length l_c, around which the nature of shock wave and fluid expansion changes, is given by

$$l_c = \frac{1+u}{1-u} d \ . \tag{5}$$

The rapidity distributions of secondary particles in evf are

$$\frac{dN_i}{d\eta} = -\pi a_\pi{}^2 s_0 \frac{n_c}{s_c} \exp\left[\left(\frac{1-u^2}{u^2}\right)\tau_c\right] \times u^2 \frac{\partial}{\partial \tau}\left(\frac{\partial \Phi_i}{\partial \tau} - \Phi_i\right)\Big|_{\tau=\tau_c} , \tag{6}$$

where $i = 1$ corresponds to the target with $l \leq l_c$ and $i = 2$ to the target with $l > l_c$. η is the rapidity in evf, $\tau_c = \ln(T_c/T_0)$, and Φ_i are the solutions of the so-called nontrivial region of fluid as is discussed in II. s_0 and T_0 are the entropy density and temperature respectively of the fluid after the shock wave passes but before the expansion starts; s_c, n_c, and T_c are the critical entropy density, number density, and temperature respectively at which particles emerge from the fluid. The rapidity distributions $dN_i/dY_{\rm lab}$ in the laboratory frame at 200 GeV can be obtained from Eq. (6) with a boost to the forward direction by $\Delta\eta = 3.03$.

In our hydrodynamical theory various parameters are determined by normalizing the total number $N_{\rm total}$ of secondary particles produced in proton-proton collision at a given energy to a certain number which is supposed to be determined from experiment. The connection between the observed charged multiplicity $N^{\rm ch}$ of proton-proton collision, which also contains an initial two protons, and $N_{\rm total}$, which contains only secondary particles, is not clearly established at present.

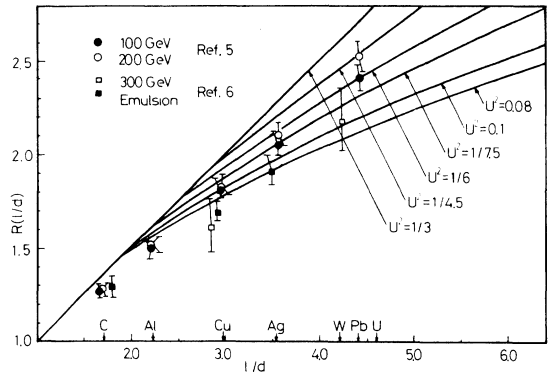

FIG. 1. Prediction of the one-dimensional hydrodynamical model for the multiplicity ratio $R(l/d)$ as a function of u and l/d. The corresponding values of l/d according to Eqs. (2)–(4) for several representative nuclei are shown by arrows.

In this paper we employ the formula used by Chadha, Lam, and Leung,[8]

$$N^{\rm ch} = n^{\rm ch} + \tfrac{4}{3} \ , \tag{7}$$

where $n^{\rm ch}$ is the total number of charged secondaries. From Eq. (7) we obtain the relation between $N^{\rm ch}$ and $N_{\rm total}$ (in the approximation that all secondaries are pions) as

$$N_{\rm total} = \tfrac{3}{2} N^{\rm ch} - 2 \ . \tag{8}$$

Using Eq. (8) and $N^{\rm ch} = 7.4$ obtained by Busza *et al.*,[5] we get $N_{\rm total} = 9.1$ which will be the basis of normalization in our theoretical calculations. The total number of secondary particles for proton-nucleus collision with target tunnel length l is obtained from $R(l/d)$ in I and $N_{\rm total} = 9.1$. $R(l/d)$ in terms of the velocity of sound u and the target tunnel length l is given in Fig. 1.

The histograms in Figs. 2 and 3 are the experimental data[5] on the pseudorapidity ($\eta_{\rm ps}$) distributions of charged particles produced in the collisions of p-H_2, p-Al, p-em (emulsion), and p-Ag at 200 GeV in the laboratory frame. The continuous curves represent the hydrodynamical prediction of rapidity distributions with $u = 1/(7.5)^{1/2}$. The lower, middle, and upper curves in Fig. 2 correspond to p-H_2, p-Al, and p-Ag collisions, respectively. In order to obtain these theoretical curves from Eq. (6) which is normalized to $N_{\rm total}(l/d)$, where

$$N_{\rm total}(l/d) = N_{\rm total}(pp) R(l/d) \ , \tag{9}$$

and $R(l/d)$ can be read from Fig. 1 with $u = 1/(7.5)^{1/2}$, we multiplied Eq. (6) with 7.4/9.1, 11.2/14.7, 13.5/16.9, and 15.5/18.8 for p-H_2, p-Al, p-em, and p-Ag collisions, respectively. The numbers in the numerators represent the observed charged multiplicities (charged pions and fast pro-

tons)[5] and the numbers in the denominators represent the total numbers of secondary pions (neutral as well as charged pions) calculated from Eq. (9). The procedure adopted here therefore implies that the number of protons counted among the observed charged particles is essentially proportional to $R(l/d)$ and that their distribution is proportional to the pionic distribution as computed by the hydrodynamical model. These protons stem from the recoils and evidently correspond to all the ones participating in the collision. It is known from π^--Ne collisions according to Ref. 9 that such protons occur among the observed particles, but their spectra is, in Ref. 9, rather different from our assumption. However, this experiment corresponds to low projectile energy. In proton-nucleus collisions there are no available experimental data in this regard except for the preliminary data by Fujioka *et al.*[10]

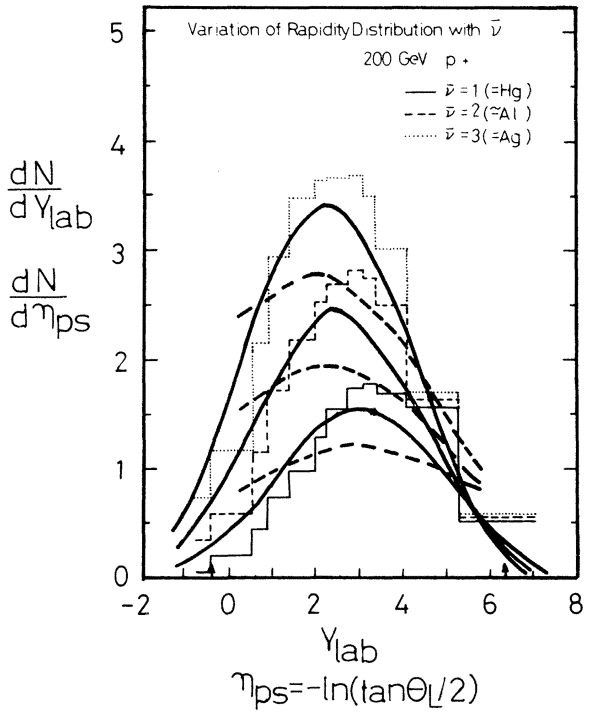

FIG. 2. Hydrodynamical predictions of rapidity distributions of secondary particles in the collision of p-H_2 ($\bar{\nu}=1$), p-Al ($\bar{\nu}=1.95$), and p-Ag ($\bar{\nu}=3$) at 200 GeV. The continuous lines are those with $u=1/\sqrt{7.5}$ and the dashed lines are those with $u=1/\sqrt{3}$. The lower, middle, and upper lines in each set correspond to p-H_2, p-Al, and p-Ag collisions, respectively. The maximum and minimum rapidities with $u=1/\sqrt{6}$ are indicated by arrows. Within these limits the distribution with $u=1/\sqrt{6}$ for p-p almost overlaps that with $u=1/\sqrt{7.5}$. The experimental data are from Ref. 5. Y_{lab} refers to the theoretical prediction and η_{ps} to the experimental data.

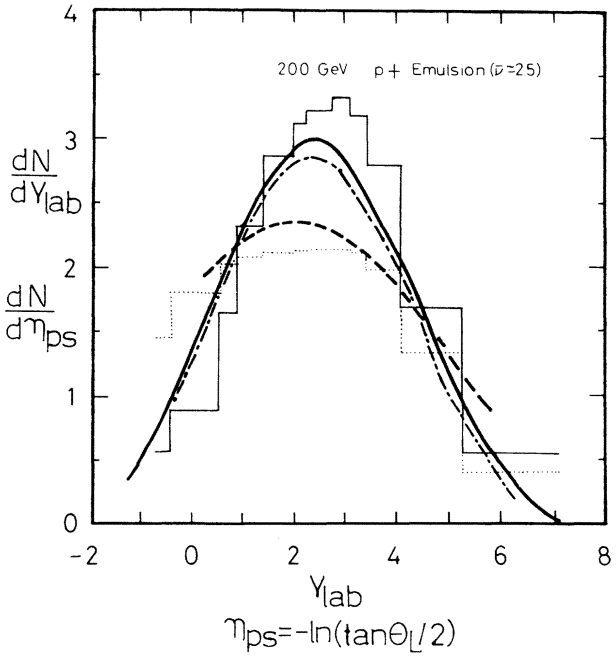

FIG. 3. The same as in Fig. 2 for p-(emulsion) ($\bar{\nu}=2.5$) collisions. The continuous line is that with $u=1/(7.5)^{1/2}$ and the dot-dashed line is that with $u=1/\sqrt{6}$. The dotted histogram refers to the prediction of the coherent tube model discussed in Ref. 5.

The value $u=1/(7.5)^{1/2}$ is the preferred value we obtain by comparing rapidity distributions of secondaries at 200 GeV and the ratio N_{pA}/N_{pp} for various A with data.[1] The energy dependence of these distributions cannot be tested at present because of a lack of data.

Andersson *et al.*[11] obtained $u\simeq 1/(6.25)^{1/2}$ from an overall fit of p-p data including rapidity distributions and their energy dependence in the range $200\leq E_{lab}\leq 1500$ GeV. In order to compare these two values of velocity of sound we computed also the rapidity distributions for p-p and p-em with $u=1/\sqrt{6}$. The results are given in Figs. 2 and 3. For p-p collisions, the two distributions almost overlap in the central region, but the rapidity region with $u=1/\sqrt{6}$ is considerably smaller than that with $u=1/(7.5)^{1/2}$. A similar comment applies to p-em distributions. Thus, the quality of our theoretical fits is determined mainly by the available rapidity range for each value of u. A comparison of theoretical rapidity ranges with the p-p data from CERN ISR experiments in the energy region $200\leq E_{lab}\leq 1500$ GeV also shows that $u=1/(7.5)^{1/2}$ is a preferred value to $u=1/\sqrt{6}$. This observation is in agreement with the results of Ref. 11, where it was found that if one considers only

the energy dependence in the p-p data, one gets a larger value of u than if one considers the rapidity range alone. Whether this slight discrepancy persists also in the p-A case will be clarified only with the appearance of p-A data at higher energies. On the other hand, it is not *a priori* necessary that the velocity of sound in nuclear hadronic matter should be identical to the velocity of sound in nucleonic hadronic matter.

The theoretical rapidity distributions of charged particles, which are expressed by continuous curves in Figs. 2 and 3, represent the contributions from only the so-called nontrivial region of fluid. The other parts of fluid regions (progressive wave regions and first reflected wave region) may contain a certain number of particles.[2] But for $u = 1/(7.5)^{1/2}$ these numbers are negligible as is demonstrated in II. The dashed lines in Figs. 2. and 3 represent the hydrodynamical predictions with $u = 1/\sqrt{3}$. In order to obtain the theoretical rapidity distributions of charged particles for $u = 1/\sqrt{3}$ from Eq. (6), we multiplied Eq. (6) with 7.4/9.1, 11.2/14.7, 13.5/17.8, and 15.5/20.7 for p-H_2, p-Al, p-em, and p-Ag, collisions respectively. The numbers in the denominators are obtained from Eq. (9) with $u = 1/\sqrt{3}$. Unlike the case of $u = 1/(7.5)^{1/2}$, the number of particles contained in the progressive wave and first reflected wave regions for $u = 1/\sqrt{3}$ are not negligible. They are 1.5, 2.3, 2.8, and 3.2 for p-H_2, p-Al, p-em, and p-Ag collisions, respectively. The particles in the progressive wave regions tend to fill the gaps at both ends of the distribution.[2] Thus the number of particles contained under each dashed curve in Figs. 2 and 3 plus the corresponding number in the other fluid regions given above should correspond to the observed charged multiplicity.

The hydrodynamical prediction of dN/dY_{lab} for $u = 1/\sqrt{3}$ is evidently not acceptable so that we will not discuss this case in the following. On the other hand, the hydrodynamical prediction of dN/dY_{lab} for $u = 1/(7.5)^{1/2}$ is quite reasonable, particularly in view of the fact that we are not doing any least-χ-square-type search of the best value of u to fit the data.

Comparing our theoretical predictions with the data, it seems that a systematic shift of rapidity by $\Delta Y_{\text{lab}} \sim 0.5$ would produce a better fit. But we do not have any theoretical or experimental explanation for this shift at present. Otherwise, the agreement between the experimental data and the theoretical predictions is excellent. This refers to (1) the shape of distribution, (2) the maximum and minimum values of rapidities, (3) the fact that there is no increase of number of particles in the very forward region, (4) the target-dependent increase of the number of particles in the backward region, and (5) the shift of peak positions to the backward as the target size increases.

The fit to the data in the backward region can probably be improved by doing a least-χ-square search for the best values of free parameters, but this is beyond the scope of the present paper since we do not have the data with their errors.

It should also be noted here that in our calculation the three-dimensional motion and viscosity are neglected. A study by Andersson *et al.*[11] indicates that the velocity of sound determined from the three-dimensional formula and that from the one-dimensional formula for negatively charged secondaries are both about $u \sim 1/(6.25)^{1/2}$, but that the critical temperatures differ substantially in the two cases, and our result on the critical temperature is close to that from the three-dimensional formula.

Whether the discrepancy between the critical temperatures derived in the present work and those obtained from the one-dimensional formula by Andersson *et al.* is significant is not clear since in our approach T_c is a function of u while Andersson *et al.* assume that both u and T_c are free parameters.

In order to compare the predictions of other theoretical models with the data, we first summarize general properties which can be derived from various theoretical rapidity distributions of secondary particles. The energy-flux-cascade model[12] (EFCM) predicts that the excess number of secondary particles in proton-nucleus collisions over proton-proton collision should be concentrated in the backward third of the rapidity region. In the remaining (middle and forward) two rapidity regions there are no changes of the numbers of secondary particles over proton-proton collisions. The coherent-production model (CPM) of Fishbane and Trefil[13] predicts that the excess number of secondary particles of proton-nucleus collision over proton-proton collision should be concentrated in the backward half of the rapidity region. The two-phase model (TPM)[14] and the multiperipheral model (MPM)[15] predict an increase of the number of secondary particles in proton-nucleus collision as compared with proton-proton collision in the whole rapidity region, but the increase at the minimum rapidity is largest and it becomes gradually smaller as one approaches the maximum rapidity. On the other hand, the hydrodynamical model (HDM) predicts that in the very forward rapidity region ($Y_{\text{lab}} \geq 5.5$) the excess number of secondary particles is negative,[16] and for the remaining region $Y_{\text{lab}} < 5.5$ the excess number gradually increases as one approaches the backward rapidity region. From Fig. 4 we conclude that if we average the excess numbers over the rapidity region

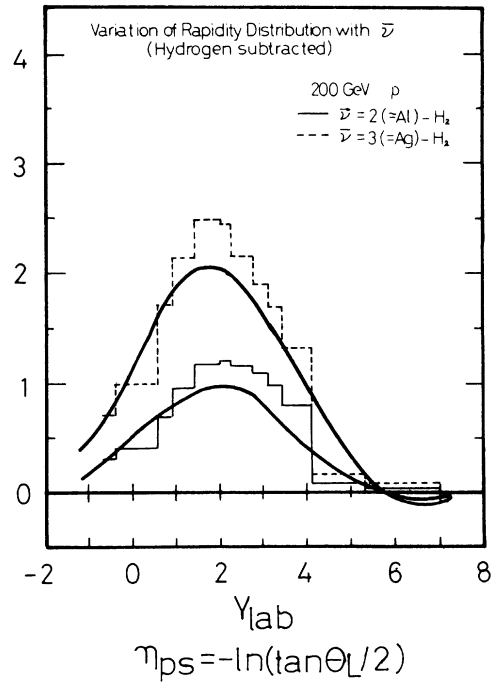

FIG. 4. Hydrodynamical prediction of rapidity distributions of p-Al and p-Ag collisions at 200 GeV after subtracting the p-H_2 distribution.

from $Y_{lab} = 4.75$ to $Y_{lab} = 7$, we get practically zero.

The comparison of the above predictions of various theoretical models with the data does not favor EFCM and CPM since these two models predict a zero excess number in the forward region ($Y_{lab} \geq 3.03$) while the data in Fig. 4 show a positive excess number in the same region. The same is true for TPM and MPM since these models predict the positive excess number in the entire rapidity region while the data show an almost zero excess number for $Y_{lab} \geq 5.3$. On the other hand, the HDM seems to agree with the data in this last respect since it predicts the zero excess number on the average in the region $Y_{lab} \geq 5.0$, although more detailed experimental data in the very forward region are needed to draw a definite conclusion. We have already pointed out that the shift of peak positions of the rapidity distribution with increasing target size as predicted by HDM is consistent with the data as is shown in Fig. 2. But this shift is not accounted for by the EFCM and TPM.

Finally we should point out that another possible criterion for the test of various models is to measure the average rapidity $\langle\eta\rangle$, the average rapidity in the backward region $\langle\eta_b\rangle$, and the average rapidity in the forward region $\langle\eta_f\rangle$ of secondary particles in the evf. For example, in EFCM and CPM $\langle\eta_f\rangle$ remains constant as the target size increases. $\langle\eta_b\rangle$ and $\langle\eta_f\rangle$ in TPM, MPM and HDM should decrease as the target size increases but the rate of decrease of $\langle\eta_f\rangle$, for example, should be different in TPM, MPM, and HDM. $\langle\eta_f\rangle$ in HDM should show a faster decrease than in TPM and MPM since the rapidity distribution in the very forward region in HDM actually decreases with increasing target size. In II many other interesting effects in proton-nucleus collision were predicted, which need new experimental data for comparison. The analysis of the pion-nucleus data[5] makes necessary a modification of the calculations performed in II. This will be the subject of a future publication.

We conclude that the HDM can explain in a satisfactory way the experimental rapidity distribution in proton-nuclues collisions.

Note added. The data on p-Cr and p-W collisions at 300 GeV given in Ref. 6 are fitted in Figs. 5(a) and 5(b) with our model using the same parameters as in the case of 200 GeV except the incident energies and target sizes. In each case we fitted the

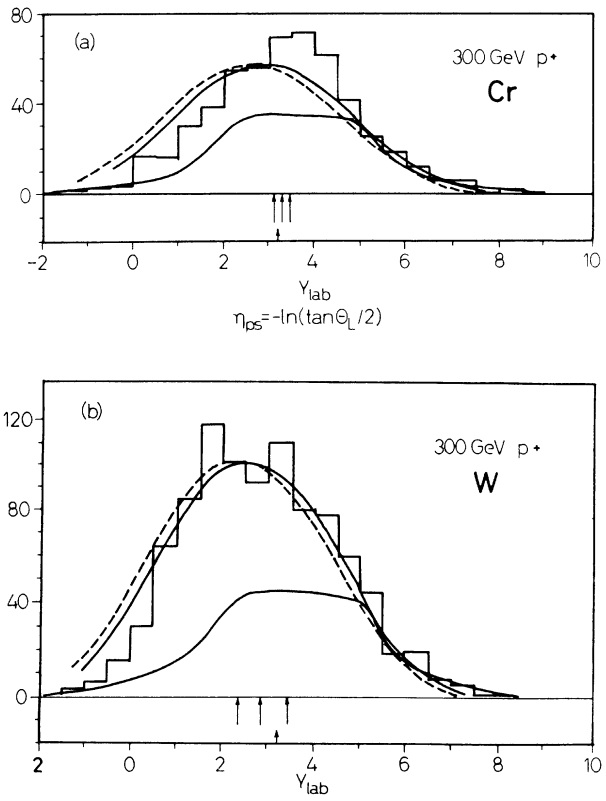

FIG. 5. Data on p-Cr and p-W collisions at 300 GeV (Ref. 6) fitted with our model. The unit of the data is the number of counts of tracks. The dashed line represents our theoretical fit and the solid line is our fit shifted (see note added). The symmetrical line represents the 205-GeV hydrogen data scaled to 300 GeV.

data by normalizing the total number of secondaries in our model to the total area of the histogram. The dashed line represents our theoretical fit and the continuous one is the result of uniform shift of our result by $\Delta Y_{\text{lab}} = 0.23$ to the positive direction. This shift seems necessary since the centroid (the arrow in the far right among three arrows) of p-p determined in Ref. 6 does not coincide with the true centroid determined from an exact kinematical calculation (the arrow in the bottom). Thus, instead of shifting the data to the negative direction we shifted our theoretical result to the positive direction by the same amount. See the text for more detail of the method of our fit.

The authors would like to thank Professor W. Busza of M.I.T. for sending us a report on the experimental data quoted in this paper. One of the authors (N. Masuda) would like to thank Professor F. Cerulus and other members of the Institute for Theoretical Physics, University of Leuven, for their hospitality. This work was supported in part by the Deutsche Forschungsgemeinschaft.

---

*Now at Physics Laboratory, Education Faculty, Yamagata University, Yamagata, Japan 990.

[1]N. Masuda, Phys. Rev. D 15, 1314 (1977).

[2]N. Masuda and R. M. Weiner, Phys. Rev. D 18, 1515 (1978).

[3]L. D. Landau, Izv. Akad. Nauk (USSR) 17, 51 (1953).

[4]S. Z. Belenkij and G. A. Milekhin, Zh. Eksp. Teor. Fiz. 29, 20 (1955) [Sov. Phys.—JETP 2, 14 (1956)].

[5]W. Busza, D. Luckey, L. Votta, C. Young, C. Halliwell, and J. Elias, paper submitted to the XVIII International Conference on High Energy Physics, 1976 (unpublished).

[6]J. R. Florian, M. Y. Lee, J. J. Lord, J. W. Martin, R. J. Wilkes, R. E. Gibbs, and L. D. Kirkpatrick, Phys. Rev. D 13, 558 (1976).

[7]J. Babechi *et al.*, Phys. Lett. 47B, 268 (1973); A. Gurtu *et al.*, *ibid.* 50B, 391 (1974); R. E. Gibbs *et al.*, Phys. Rev. D 10, 783 (1974); P. L. Jain *et al.*, Phys. Rev. Lett. 33, 660 (1974); Alma-Ata-Leningrad-Moscow-Tashkent Colloboration, Yad. Fiz. 19, 1046 (1974) [Sov. J. Nucl. Phys. 19, 536 (1974)]; Barcelona-Batavia-Belgrade-Bucharest-Lund-Lyons-Montreal-Nancy-Ottawa-Paris-Rome-Strasborg-Valencia Collaboration, Phys. Lett. 48B, 467 (1974).

[8]S. Chadha, C. S. Lam, and Y. C. Leung, Phys. Rev. D 10, 2817 (1974).

[9]J. R. Elliott *et al.*, Phys. Rev. Lett. 34, 607 (1975).

[10]G. Fujioka *et al.*, J. Phys. Soc. Jpn. 39, 1131 (1975).

[11]B. Andersson, G. Jarlskog, and G. Damgaard, Nucl. Phys. B112, 413 (1976).

[12]K. Gottfried, Phys. Rev. Lett. 32, 957 (1974).

[13]P. M. Fishbane and J. S. Trefil, Phys. Rev. D 9, 168 (1974).

[14]P. M. Fishbane and J. S. Trefil, Phys. Lett. 51B, 139 (1974).

[15]J. Koplick and A. H. Mueller, Phys. Rev. D 12, 3638 (1975).

[16]This result seems consistent with the recent data by L. J. Gutay, A. T. Laasanen, C. Ezell, W. N. Schreiner, and F. Turkot, Phys. Rev. Lett. 37, 468 (1976).

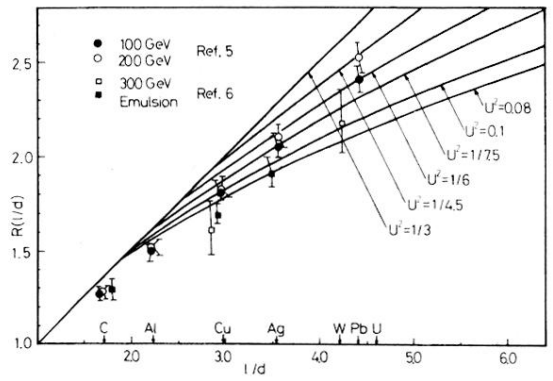

FIG. 1. Prediction of the one-dimensional hydrodynamical model for the multiplicity ratio $R(l/d)$ as a function of u and l/d. The corresponding values of l/d according to Eqs. (2)–(4) for several representative nuclei are shown by arrows.

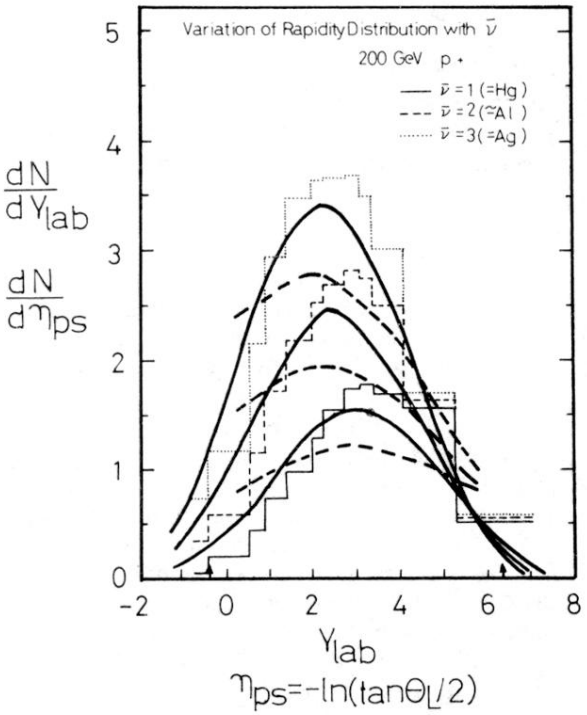

FIG. 2. Hydrodynamical predictions of rapidity distributions of secondary particles in the collision of p-H_2 ($\bar{\nu}=1$), p-Al ($\bar{\nu}=1.95$), and p-Ag ($\bar{\nu}=3$) at 200 GeV. The continuous lines are those with $u=1/\sqrt{7.5}$ and the dashed lines are those with $u=1/\sqrt{3}$. The lower, middle, and upper lines in each set correspond to p-H_2, p-Al, and p-Ag collisions, respectively. The maximum and minimum rapidities with $u=1/\sqrt{6}$ are indicated by arrows. Within these limits the distribution with $u=1/\sqrt{6}$ for p-p almost overlaps that with $u=1/\sqrt{7.5}$. The experimental data are from Ref. 5. Y_{lab} refers to the theoretical prediction and η_{ps} to the experimental data.

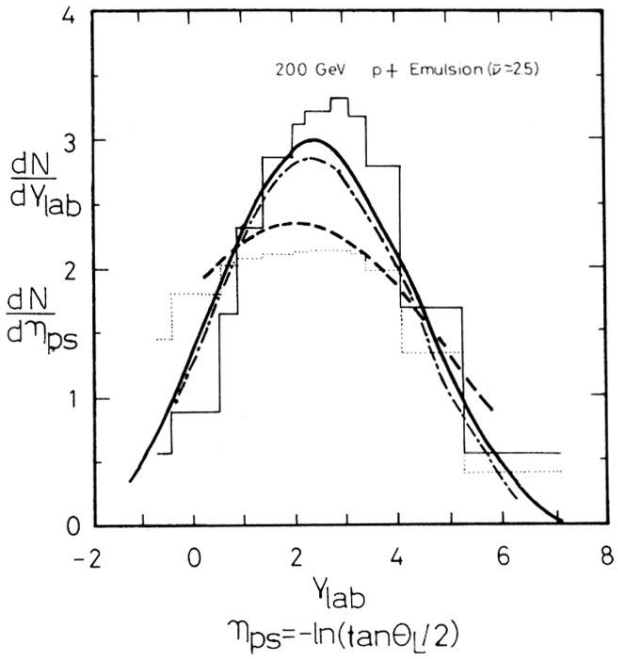

FIG. 3. The same as in Fig. 2 for p-(emulsion) ($\bar{\nu}$ = 2.5) collisions. The continuous line is that with u = $1/(7.5)^{1/2}$ and the dot-dashed line is that with $u = 1/\sqrt{6}$. The dotted histogram refers to the prediction of the coherent tube model discussed in Ref. 5.

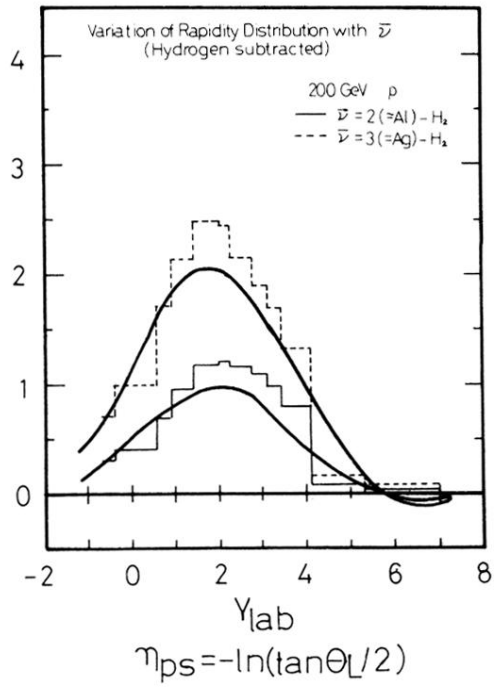

FIG. 4. Hydrodynamical prediction of rapidity distributions of p-Al and p-Ag collisions at 200 GeV after subtracting the p-H_2 distribution.

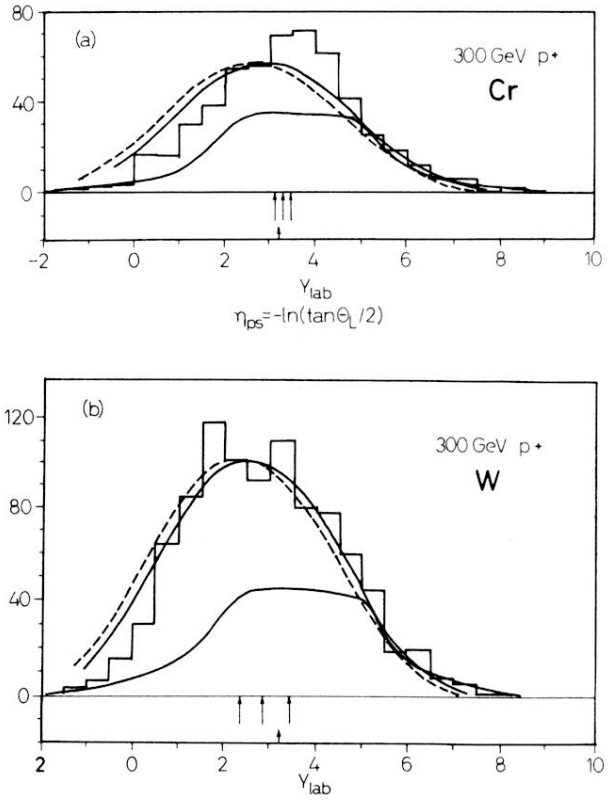

FIG. 5. Data on p-Cr and p-W collisions at 300 GeV (Ref. 6) fitted with our model. The unit of the data is the number of counts of tracks. The dashed line represents our theoretical fit and the solid line is our fit shifted (see note added). The symmetrical line represents the 205-GeV hydrogen data scaled to 300 GeV.